Supporting information for

Chiral metal-organic frameworks with tunable open channels as single-site asymmetric cyclopropanation catalysts

Joseph Falkowski, Sophie Liu, Cheng Wang, and Wenbin Lin*

Department of Chemistry, CB#3290, University of North Carolina, Chapel Hill, NC 27599, USA

wlin@unc.edu

1. General experimental

All of the solvents were purchased from Fisher and used without further purification. All of the reactions and manipulations were carried out under nitrogen with the use of standard inert atmosphere and Schlenk techniques. ^{1}H NMR spectra were recorded on a Bruker NMR 400 DRX spectrometer at 400 MHz and referenced to the proton resonance resulting from incomplete deuteration of the deuterated methylene chloride (δ 5.32). ^{13}C{1H} NMR spectra were recorded at 100 MHz, and all of the chemical shifts are reported downfield in ppm relative to the carbon resonance of methylene chloride-d_2 (δ 54.00). Mass spectrometric analyses were conducted using positive-ion electrospray ionization on a Bruker BioTOF mass spectrometer. Thermogravimetric analysis (TGA) was performed in air using a Shimadzu TGA-50 equipped with a platinum pan. Single-crystal X-ray diffraction and powder X-ray diffraction (PXRD) patterns were collected on a Bruker SMART APEX II diffractometer using Cu radiation. The PXRD patterns were processed with the APEX 2 package using PILOT plug-in. Conversions and e.e. values were determined by gas chromatography (GC) using a Shimadzu GC-2010 gas chromatograph equipped with a flame ionization detector (FID). The synthesis and characterization of (*E*)-methyl 3-(3-(*tert*-butyl)-5-formyl-4-hydroxyphenyl)acrylate has been reported previously.[1] Sodium trimethoxyborohydride was purchased from Sigma-Aldrich. Abbreviations: DBF, *N*,*N*-dibutylformamide; DMF, dimethylformamide; DEF, diethylformamide; BB R-250, Brilliant Blue R-250; EDA, ethyl 2-diazoacetate; PTFE, pertetrafluoroethylene.

2. Procedure for ligand synthesis

2.1 (*R*,*R*)-*N*,*N*'-bis(3-methyl acrylate-5-*tert*-butylsalicylidene)-1,2-cyclohexanediamine (L-Me$_2$)

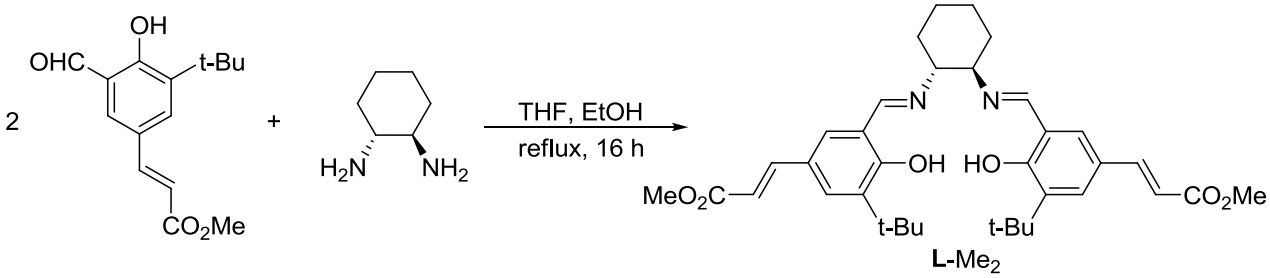

1.772 g (6.75 mmol) of (*E*)-methyl 3-(3-(*tert*-butyl)-5-formyl-4-hydroxyphenyl)acrylate was dissolved in 30 mL of tetrahydrofuran. 386 mg (3.38 mmol) of (*R*,*R*)-1,2-diaminocyclohexane was dissolved in 10 mL of ethanol. This solution was added to the THF solution and the mixture was heated to reflux overnight.

Upon cooling the reaction mixture to room temperature, the solvents were removed in vacuo. The crude product was purified by column chromatography on silica gel (ethyl acetate/triethylamine/hexanes: 9/1/90 v/v/v), and the solvents were removed under vacuum to afford a yellow powdery product of **L**-Me_2 (1.537 g, 75.5% yield). ^{1}H NMR (CD_2Cl_2): δ 1.456 (s, 18H); 1.908 (m, 2H); 1.935 (m, 2H); 2.016 (m, 2H); 3.399 (m, 2H); 3.800 (s, 6H); 6.247 (d, 2H, *J* = 15.9 Hz); 7.225 (d, 2H , *J* = 2.1 Hz); 7.480 (d, 2H, *J* = 1.8 Hz); 7.556 (d, 2H, *J* = 15.9 Hz); 8.325 (s, 2H). ^{13}C NMR (CD_2Cl_2): δ 24.420; 29.116; 32.976; 35.002; 51.540; 72.166; 114.654; 118.638; 124.287; 129.298; 130.433; 138.332; 144.625; 163.202; 165.547; 167.657.

2.2 (*R*,*R*)-*N*,*N*'-bis(3-methyl acrylate-5-*tert*-butylsalicylidene)-1,2-cyclohexanediamine dipyridyl Ruthenium(II) [Ru(L-Me_2)$(Py)_2$]

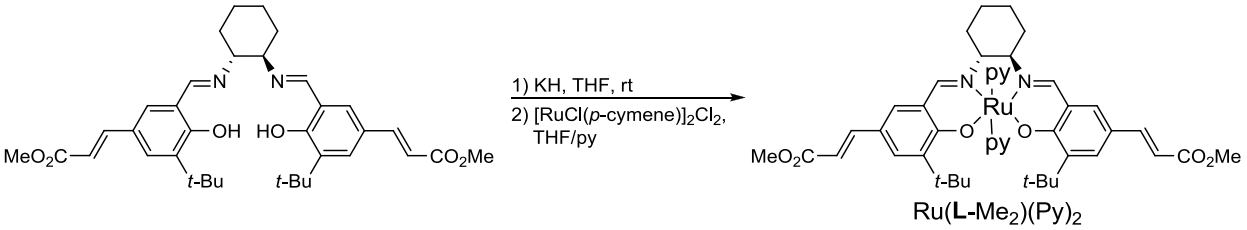

1.538 g (2.55 mmol) of **L**-Me_2 was charged into a 100 mL round-bottom flask followed by 225 mg (5.625 mmol) of potassium hydride and 30 mL of dry, degassed THF. After the evolution of hydrogen ceased, the reaction mixture was stirred under nitrogen for an additional 1 h. 854 mg (2.79 mmol) of ruthenium(*para*-cymene)dichloride was charged into a separate 100 mL round-bottom flask followed by 10 mL of dry, degassed THF and 3 mL of dry, degassed pyridine. This solution was then cooled to 0 °C. The potassium salt solution of the ligand was then added to the ruthenium(*para*-cymene)dichloride over the course of 30 min. The resulting mixture was allowed to warm to room temperature, and then to stir overnight. The solvent was removed in vacuo, and the resulting residue was purified by column chromatography (hexanes/methylene chloride/triethylamine: 49/49/2 v/v/v) to afford 1.363 g (62.1% yield) of pure maroon powdery product of Ru(**L**-Me_2)$(Py)_2$. ^{1}H NMR (CD_2Cl_2): δ 1.30 (s, 18H); 1.46 (m, 4H); 1.932 (m, 2H); 2.824 (d, 2H); 2.915 (s, 2H); 3.782 (s, 6H); 6.123 (d, 2H, *J* = 15.6 Hz); 7.066 (m, 4H); 7.387 (d, 2H, *J* = 2.4 Hz); 7.539 (m, 4H); 7.683 (d, 2H, *J* = 16.0 Hz), 8.170 (d, 4H, *J* = 5.2 Hz); 8.579 (s, 2H). ^{13}C NMR (CD_2Cl_2): δ 25.13; 29.31; 29.41; 35.80; 73.88; 109.40; 123.54; 123.81; 125.68; 134.37; 134.82; 136.58; 145.10; 146.07; 154.16; 154.83; 158.24; 168.69.

2.3 (*R*,*R*)-*N*,*N*'-bis(3-methyl acrylate-5-*tert*-butylsalicylidene)-1,2-cyclohexanediamine dipyridyl Ruthenium(III) chloride {[Ru(L)$(Py)_2$]Cl}

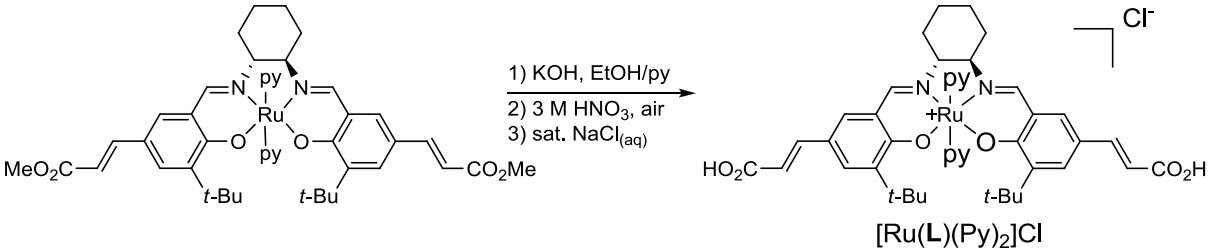

168.0 mg (0.195 mmol) of Ru(**L**)$(Py)_2$ was dissolved in 25 mL of ethanol and 1 mL of pyridine. 200 mg of KOH was then added to the degassed solution, and the mixture was stirred at reflux under nitrogen for 16 h. The reaction mixture was then cooled to room temperature, and the solvents were removed in vacuo.

The maroon powder was then dissolved in pyridine and added to 200 mL of water. With stirring, 3 M HNO_3 was slowly added to the solution until the product precipitated. The suspension was then stirred for 3 h while purging the solution with air. The resulting green solid was isolated by centrifugation. The green solid was dissolved in methanol, and 5 mL of saturated aqueous sodium chloride solution was added. The mixture was stirred overnight, and excess water was added to precipitate 131.92 mg (0.152 mmol, 78% yield) of the product Ru(**L**)$(Py)_2$]Cl as a green powder. MS (ESI) for $[M\text{-}Cl]^+$: calcd 832.28, found 832.25. $[M\text{-}Cl\text{-}py]^+$: calcd 753.24, found 753.22. $[M\text{-}Cl\text{-}2py]^+$: calcd 674.19, found 674.17.

3. Procedures for MOF synthesis

3.1 Synthesis of Zn_4O{Ru(L)$(Py)_2$]Cl}$_3$·5(DBF)·3.5(DMF) (CMOF-1)

1 mg of Ru(**L**)$(Py)_2$]Cl (1.4 µmol) and 1 mg of $Zn(NO_3)_2{\cdot}6H_2O$ (3.36 µmol) were dissolved in 0.25 mL of DBF and 0.05 mL of DMF. To this solution, 40 µL of ethanol was added. The solution was sealed in a 0.5 dram screw-cap vial and heated at 70 °C for 2 days, yielding dark green crystals (0.58 mg, 25% yield). Solvent content calculated from proposed formula: DMF, 6.7%; DBF, 20.6%. Solvent content determined by ^{1}H NMR and TGA: DMF, 6.8%; DBF 19.8%.

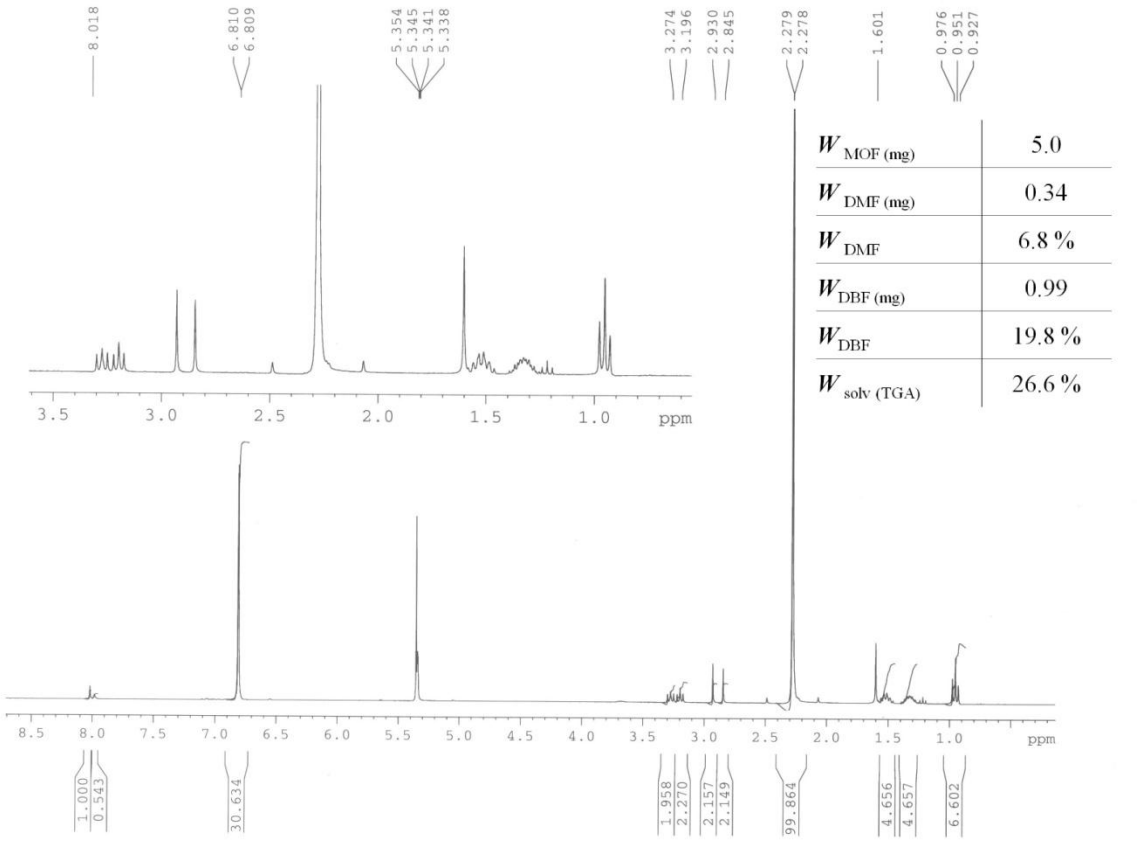

Figure S1. ^{1}H NMR solvent characterization for CMOF-**1**.

3.2 Synthesis of $Zn_4O\{Ru(L)(Py)_2]Cl\}_3$ 51(DEF) (CMOF-2)

1.0 mg (1.4 µmol) of Ru(**L**)$(Py)_2$]Cl and 1.0 mg (3.36 µmol) of $Zn(NO_3)_2{\cdot}6H_2O$ were dissolved in 0.30 mL of DEF. To this solution, 80 µL of ethanol was added. The solution was sealed in a 0.5 dram screw-cap vial and heated at 70 °C for 5 days, yielding dark green crystals (0.684 mg, 17% yield). Solvent content calculated from proposed formula: DEF, 64.2%. Solvent content determined by ^{1}H NMR and TGA: DEF, 64.3%.

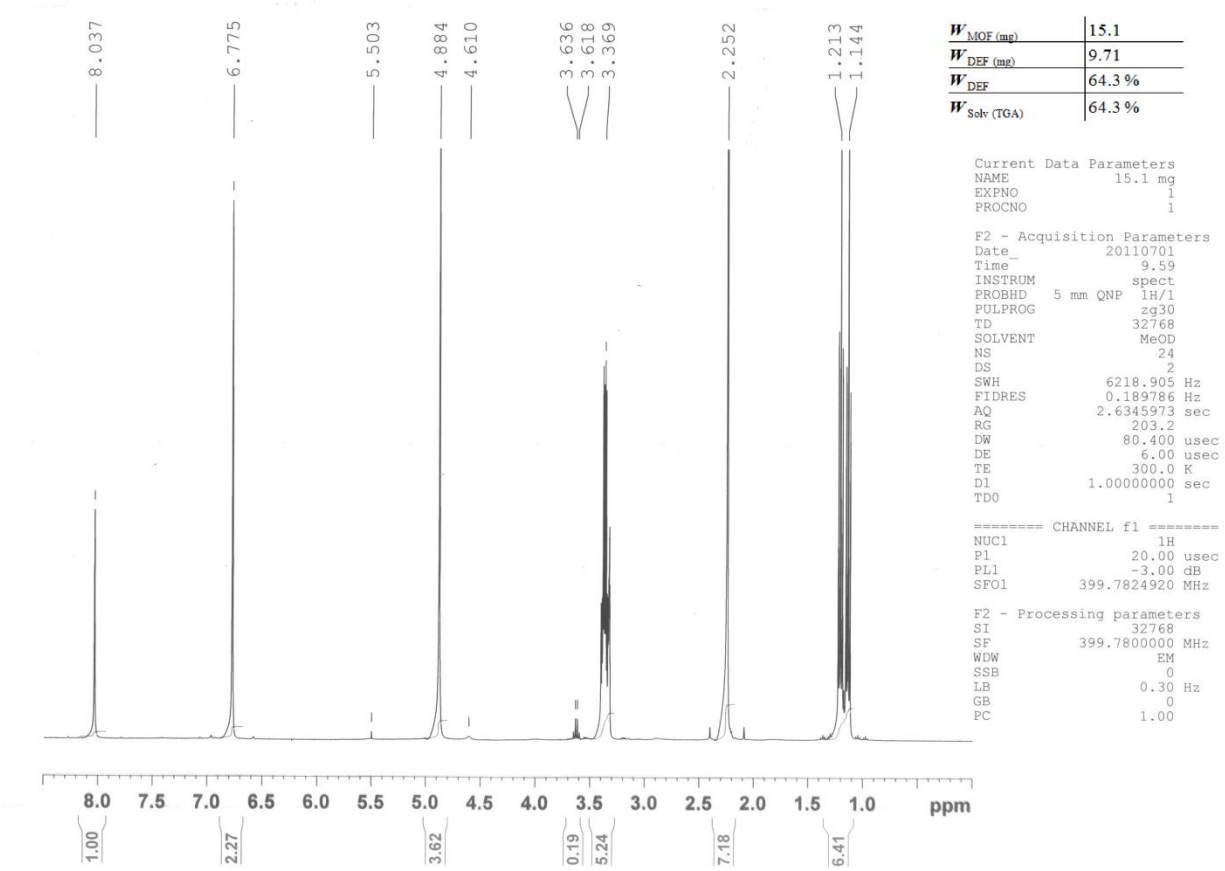

Figure S2. ^{1}H NMR solvent analysis for CMOF-**2**.

4. X-ray structure determination

All powder X-ray diffraction measurements and single crystal X-ray diffraction of CMOF-**1** were made on a Bruker SMART Apex II CCD-based X-ray diffractometer system operated at 1600 watts (Cu-target X-ray tube). The crystals were mounted inside a capillary tube (0.7 mm ID) with small amount of mother liquid to prevent solvent loss from the crystal frameworks. The frames were integrated with the Bruker

SAINT© build in APEX II software package using a narrow-frame integration algorithm, which also corrects for the Lorentz and polarization effects. Absorption corrections were applied using SADABS. Structures were solved by direct methods and refined to convergence by least squares method on F2 using the SHELXTL software suite.

For the structural refinement of CMOF-**1**, SQUEEZE subroutine of the PLATON software suite was applied to remove the scattering from the highly disordered guest molecules. The resulting new HKL4 files were used to further refine the structures. Due to the relatively weak diffraction and low resolution (>1.5 Å), which is not uncommon for this kind of framework with very large solvent accessible void space, restraints (SIMU and DELU) on displacement parameters, and DFIX for bond lengths are applied, and all the phenyl rings are constrained to ideal six-membered rings. Non-hydrogen atoms are refined isotropically. The structure solution (direct method) leads to two interpenetrating networks of full occupancy.

For CMOF-**2**, after multiple attempts of collecting single crystal X-ray diffraction data, only a dataset with a resolution of 2.1 Å was obtained (R_{int} = 0.034). The dataset was collected on a macromolecule X-ray diffraction system using a Rigaku Micromax 007HF X-ray generator (Cu rotating anode) with R-Axis IV++ detector, VariMAX HR optic and inverted Phi goniostat. The dataset contains only 763 independent reflections with 26.8% completeness. The obtained unit cell was trigonal with a = b = 36.005(3) Å, and c = 88.16(2) Å. Structure solution using direct methods in the *R*3 space group gives the coordinates of the Zn_4 cluster unambiguously. The Ru metal appears at two positions as a result of rotational disorder of the linear dicarboxylate ligand. Other parts of the organic ligands can be identified from the differential electron density map, which exhibited electron density residues at positions that connect the adjacent Zn_4 clusters (Figure S6). However, because of the poor quality of the dataset, the organic ligand cannot be resolved at atomic level. The identified positions of Zn_4 cluster and Ru metals in the structure verified that CMOF-**2** adopts a non-interpenetrated structure with the **pcu** topology. Further refinement of the structure was not performed because of low data/parameter ratios. The complete structural model was built using Materials Studio 5.5 software package.

Furthermore, Powder X-ray Diffraction patterns of CMOF-**2** was compared with that of an isostructral Mn-Salen based MOF with the same ligand length/geometry and structural topology, which we reported previously[1] (Fig. S10). The similarity of the peak positions of the two patterns supported the structural model obtained from the single crystal X-ray diffraction dataset.

Table S1. Crystal data and structure refinements for CMOFs-**1** and -**2**.

Compound	*CMOF-**1***	*CMOF-**2***
Empirical formula	$[Zn_4(\mu_4\text{-}O)\{[Ru\mathbf{L}(Py)_2]Cl\}_3]_2\cdot 10DBF\cdot 7DMF$	$[Zn_4(\mu_4\text{-}O)\{[Ru\mathbf{L}(Py)_2]Cl\}_3]$ 51DEF
Formula weight	7803.65	7410.9
Temperature (K)	296	296
Wavelength (Å)	1.54178	1.54178
Crystal system	Trigonal	Trigonal
Space group	*R*32	*R*3
Unit cell dimensions	a = 35.140(2) b = 35.140(2) c = 92.240(8) α = 90 β = 90 γ =120	a = 36.005(3) b = 36.005(3) c = 88.16(2) α = 90 β = 90 γ =120
Volume ($Å^3$)	98640(11)	98971(26)
Z	3	3
Density (calcd. g/cm^3)	0.530	0.264
Absorption coeff. (mm^{-1})	1.623	0.809
F(000)	15360	7680
Crystal size (mm)	0.40×0.40×0.40	0.20×0.20×0.20
Crystal color & shape	Brown cube	Brown cube
Radiation source	Cu Kα	Cu Kα
θ range data collection	1.4 – 26.9	3.78 – 22.60
Limiting indices	-20 < *h* < 20 -19 < *k* < 20 -53 < *l* < 53	2 < *h* < 17 -17 < *k* < -2 -14 < *l* < 24
Reflections collected	21982	1865

Independent reflections	4551	763
R(int)	0.082	0.034
Refinement method	Full-matrix least-square on F^2	
Data/restraints/parameters	4551/394/289	
Goodness-of-fit on F^2	1.72	
Final R indices $[I>2\sigma(I)]^{a,b}$	R1 = 0.1326 wR2 = 0.3182	
R indices (all data)	R1 = 0.1845 wR2 = 0.3482	

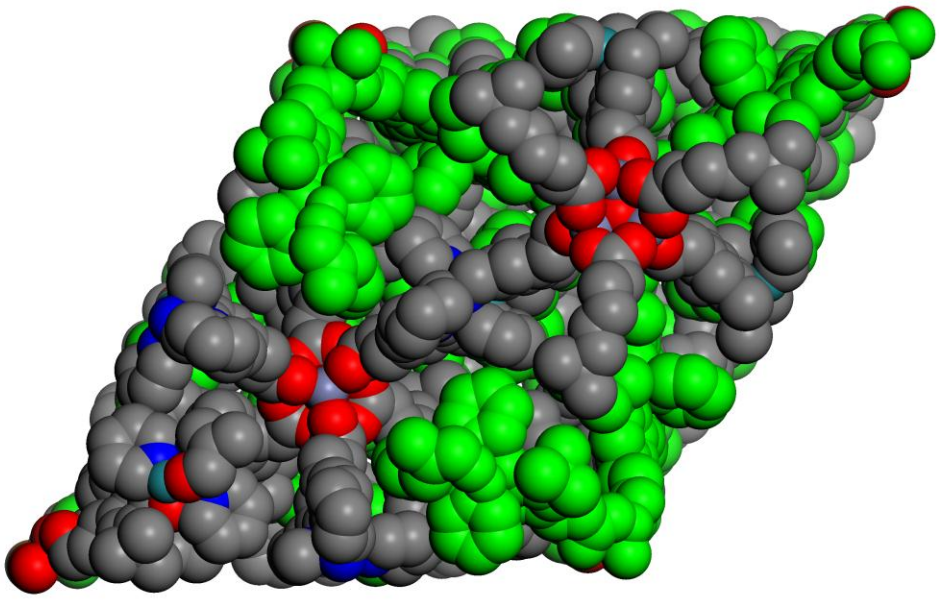

Figure S3. Space filling model of CMOF-1, viewed from [001] direction

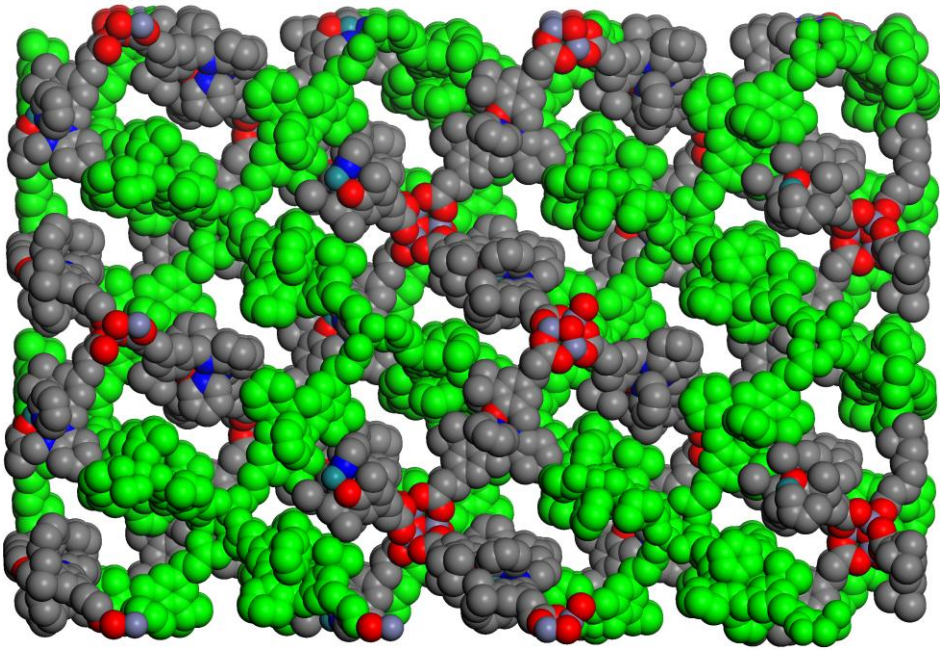

Figure S4. Space filling model of CMOF-1, viewed from [010] direction

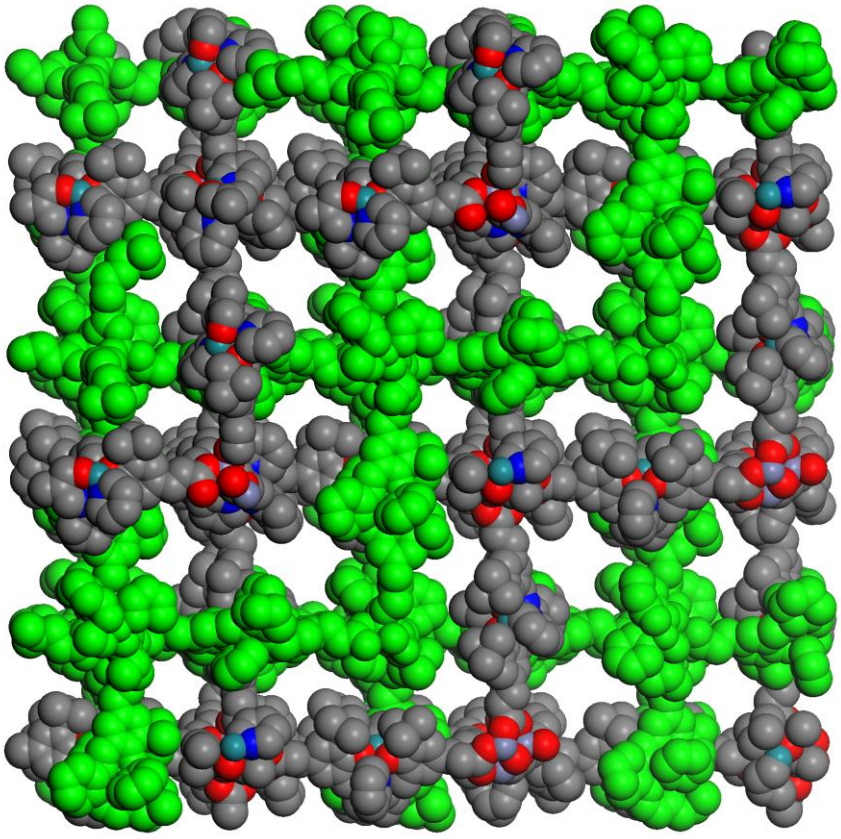

Figure S5. Space filling model of CMOF-1, viewed from [10-2] direction

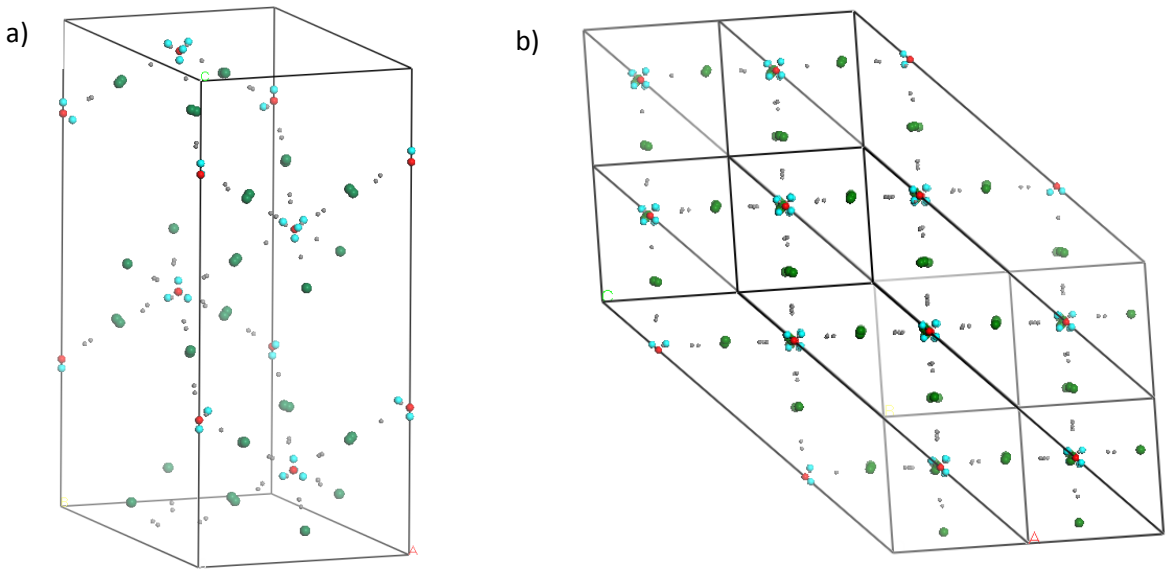

Figure S6. Incomplete structure of CMOF-**2**, showing Zn atoms (cyan ball), oxygen atoms (red ball), Ru atoms (green ball) and Q1-Q10 residue peaks (grey ball). (a) one unit cell; (b) from [1 0 -2] direction, showing non-interpenetrated structure.

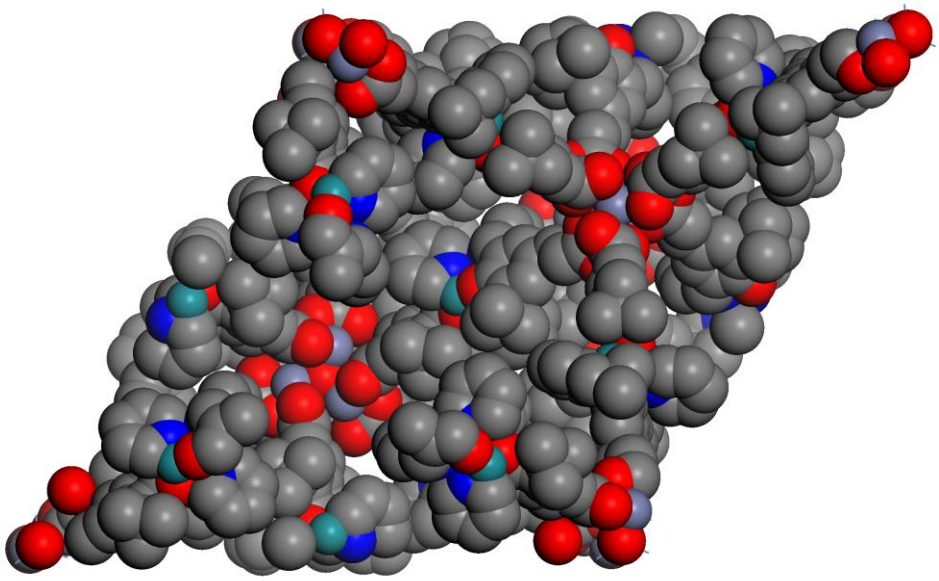

Figure S7. Space-filling model of CMOF-**2**, viewed from [001] direction.

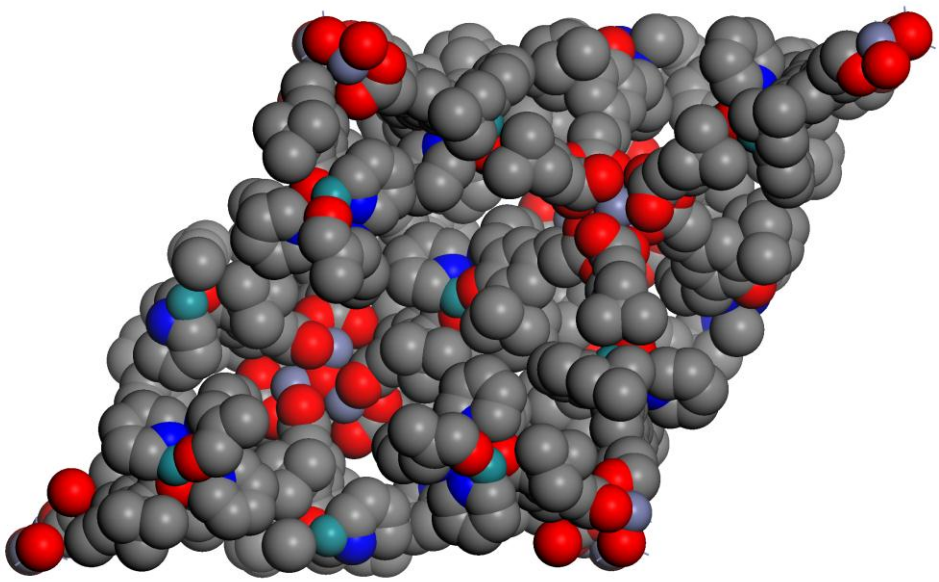

Figure S8. Space filling model of CMOF-2, viewed from [001] direction

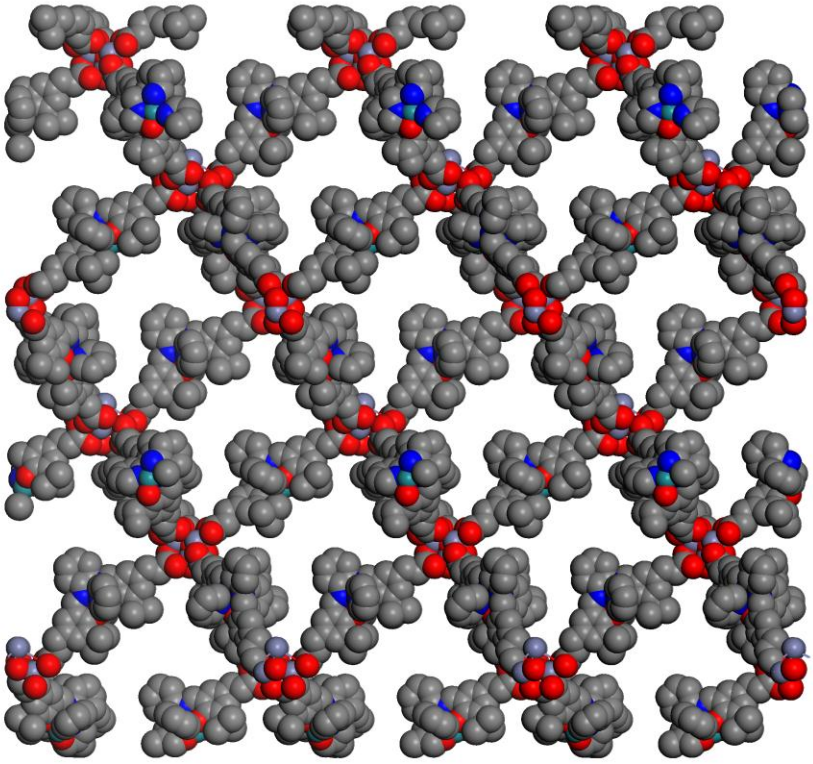

Figure S9. Space filling model of CMOF-2, viewed from [010] direction

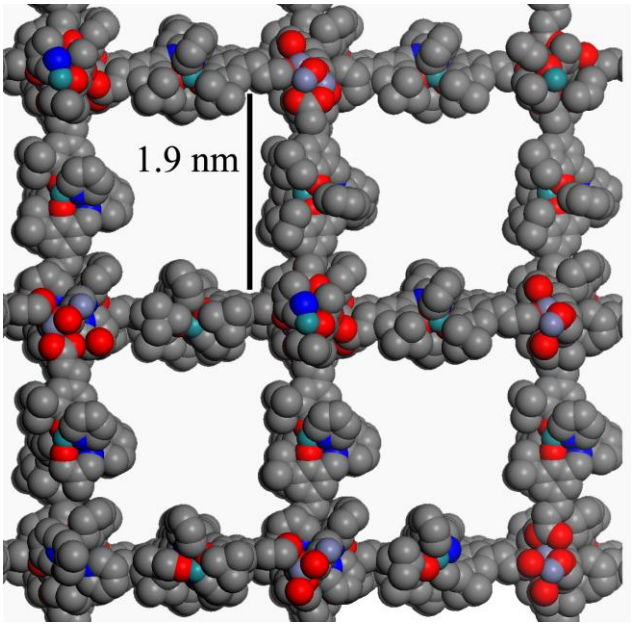

Figure S10. Space filling model of CMOF-2, viewed from [10-2] direction

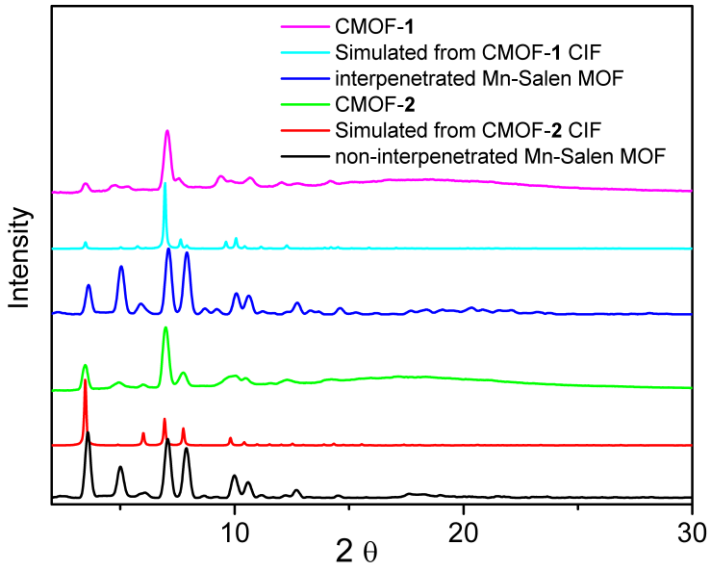

Figure S11. Comparison of Powder X-ray Diffraction patterns of CMOF-**1** and -2 with those of the isostructural Mn-Salen CMOFs we reported previously with the same ligand length/geometry and structural topology.[1]

5. Procedure for dye uptake measurements

Fresh crystals of CMOF-**2** (3.0 mg, 0.38 μmol) were briefly dried on filter paper and soaked in a methanol solution of BB R-250 (24.2 mM, 0.5 mL) for 16 h. The crystals were washed with water until the washings became colorless. The solids were then digested by Na_2EDTA (0.050 M, 2.0 mL) and NaOH (6 M, 0.1 mL). The resultant clear solution was diluted to 25 mL with water and adjusted to a pH

of 1.2 with 3 M HCl. Absorbance experiments were performed on a Shimadzu UV-2401PC UV-VIS spectrometer. The concentration of BB R-250 was determined by comparing the UV-Vis absorption with a standard curve.

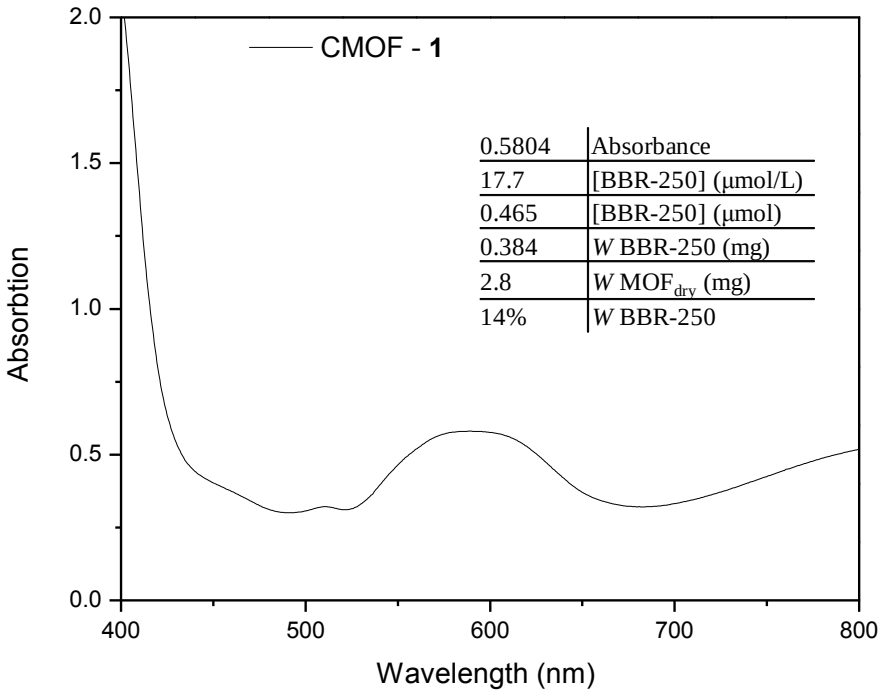

Figure S12. UV-Vis measurement of released BBR-250 from CMOF-**1**.

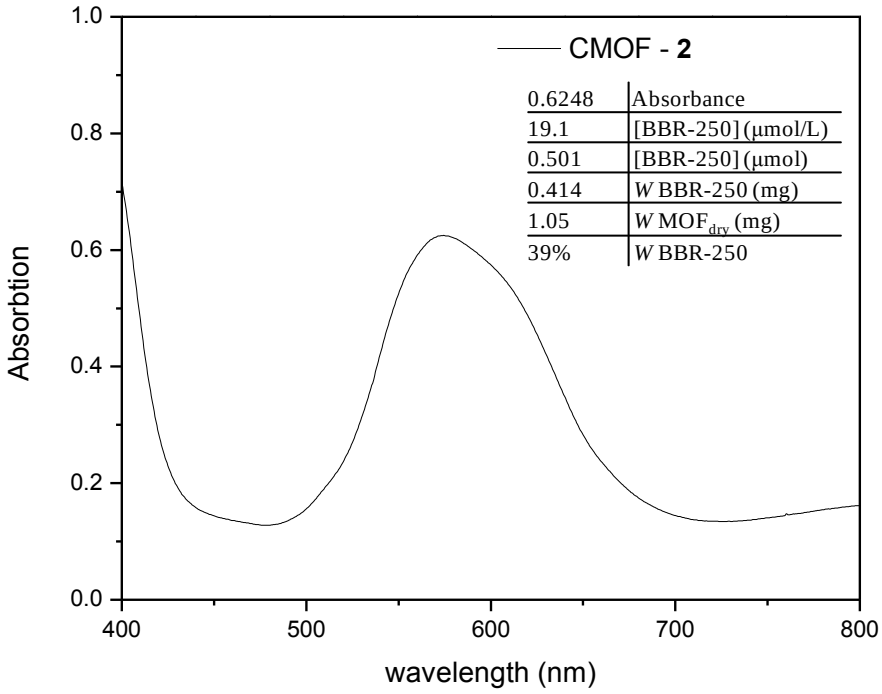

Figure S13. UV-Vis measurement of released BB R-250 from CMOF-**2**.

6. Spectroscopic characterization of reduced species

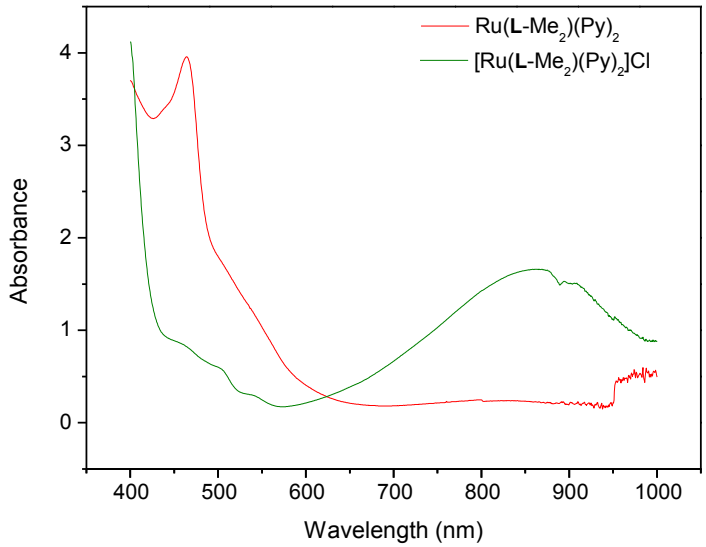

Figure S14. Vis-NIR measurements of Ru^{II}(**L**-Me_2)$(Py)_2$ and Ru^{III}(**L**-Me_2)$(Py)_2Cl$ in methanol.

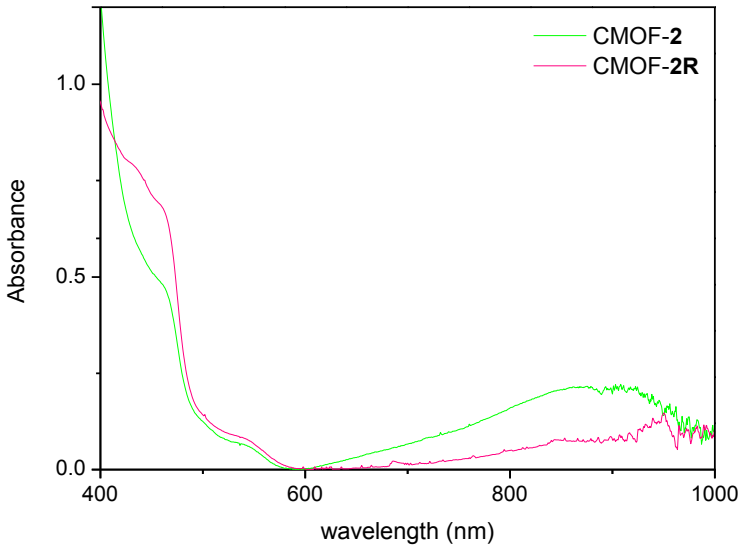

Figure S15. Solution-state Vis-NIR spectra of CMOF-**2** and CMOF-**2R** dissolved in methanol.

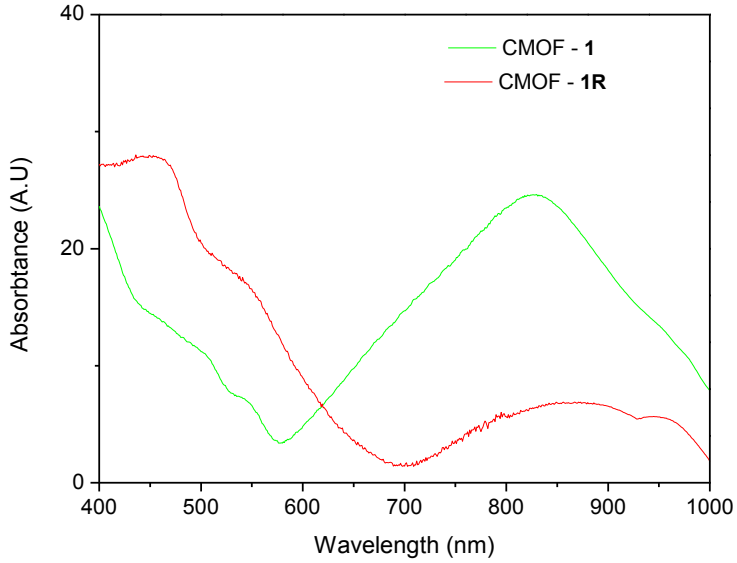

Figure **S16**. Diffuse reflectance Vis-NIR spectra of CMOF-**1** before and after reduction

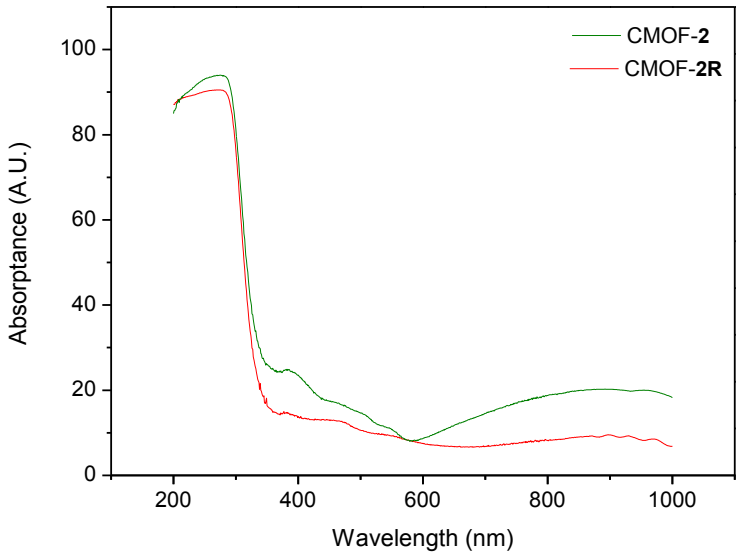

Figure S17. Diffuse reflectance Vis-NIR spectra of CMOF-**2** before and after reduction

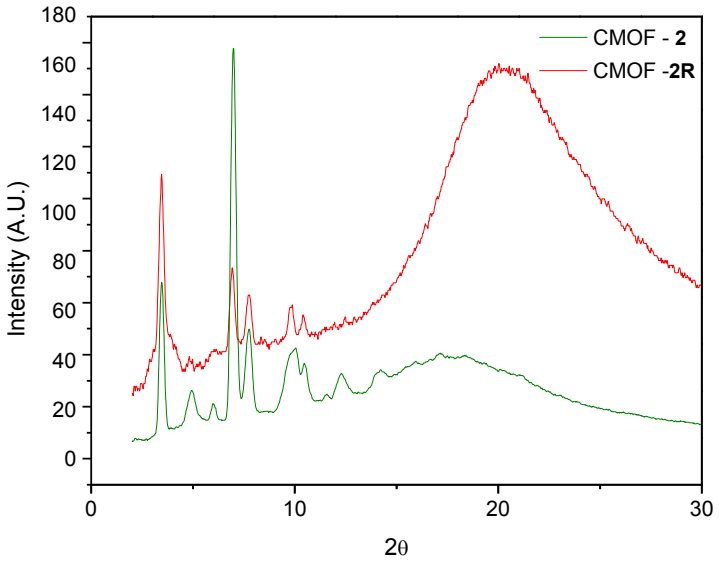

Figure S18. PXRD pattern of CMOF-**2R**. The broad peak at ~20 $^{o}2\theta$ results from the glass capillary used for mounting the sample.

7. Asymmetric cyclopropanation reactions

Carbene transfer with MOF: Fresh CMOF-**2** (8.0 mg, 0.95 µmol) was weighed out and washed with methylene chloride. The MOF was then suspended in 50 mL of methylene chloride. The suspension was vigorously purged with nitrogen gas. After 1 h, a solution of 20 mg of $NaB(OMe)_3H$ in 1 mL of dichloromethane was added to the degassing solution. After one additional hour, styrene (225 µL, 1.96 mmol) was added, and the solution was degassed for an additional hour. An undecane internal standard was added, followed by the addition of EDA (15 µL, 142 µmol). The solution was sealed and stirred overnight. The reaction mixture was then filtered through a 0.45 µm PTFE filter and then analyzed by gas chromatography.

Styrene: Supelco β-dex 120 (30 m × 0.25 mm × 0.25 µm); injector: 250 °C; column: 100-140 °C @ 0.5 °/min; detector: 250 °C; carrier gas: He (1.54 mL/min): t_1 = 58.97 min; t_2 = 60. 34 min; t_3 = 64.64 min; t_4 = 65.44 min.

Ethyl vinyl ether: Supelco β-dex 225 (30 m × 0.25 mm × 0.25 µm); injector: 250 °C; column: 80-170 °C @ 1 °/min; detector: 250 °C; carrier gas: He (1.54 mL/min): t_1 = 12.807 min; t_2 = min 12.961; t_3 = 14.671 min; t_4 = 14.798 min.

1,3-Pentadiene: Supelco β-dex 225 (30 m × 0.25 mm × 0.25 µm); injector: 250 °C; column: 70-140 °C @ 1 °/min; detector: 250 °C; carrier gas: He (1.54 mL/min): t_1 = 19.003 min; t_2 = min 19.294; t_3 = 22.038 min; t_4 = 22.454 min.

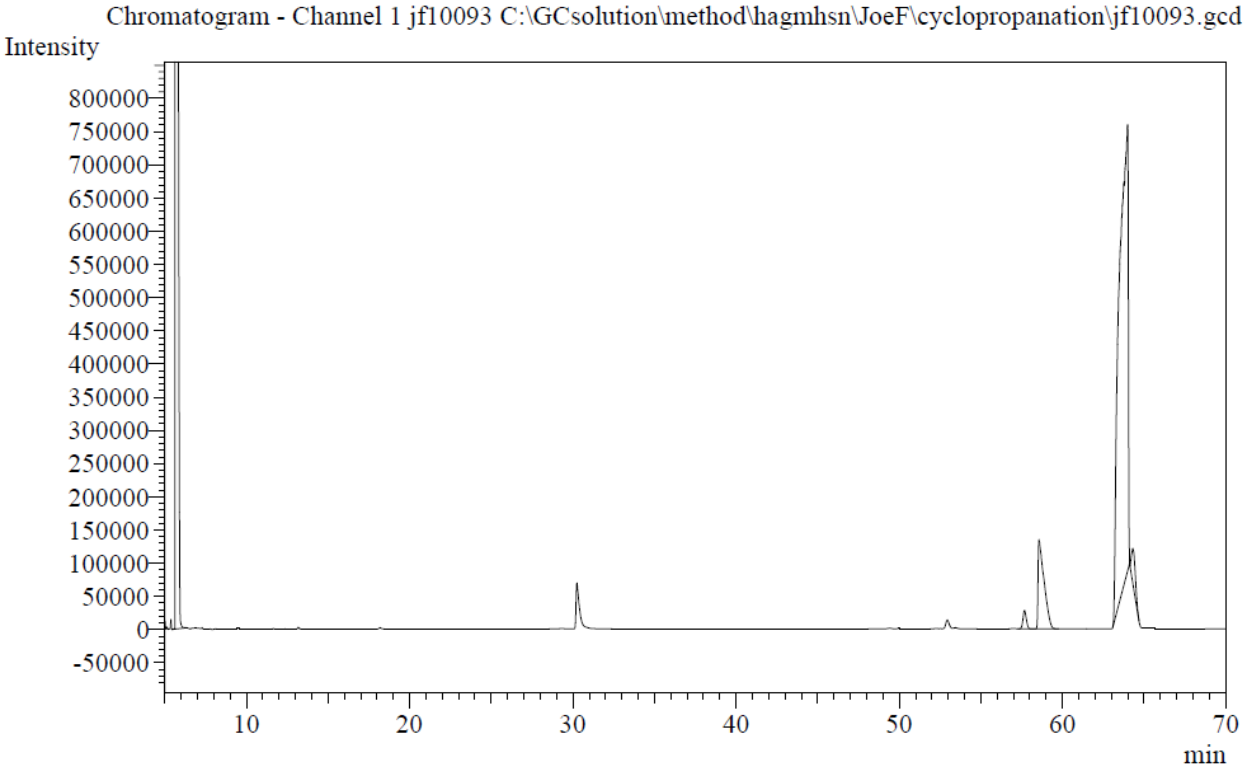

Figure S19. Cyclopropanation of styrene catalyzed by CMOF-**1R**. *Cis* e.e.: 80%; *trans* e.e.: 93%; yield: 40%; d.r.: 7.1.

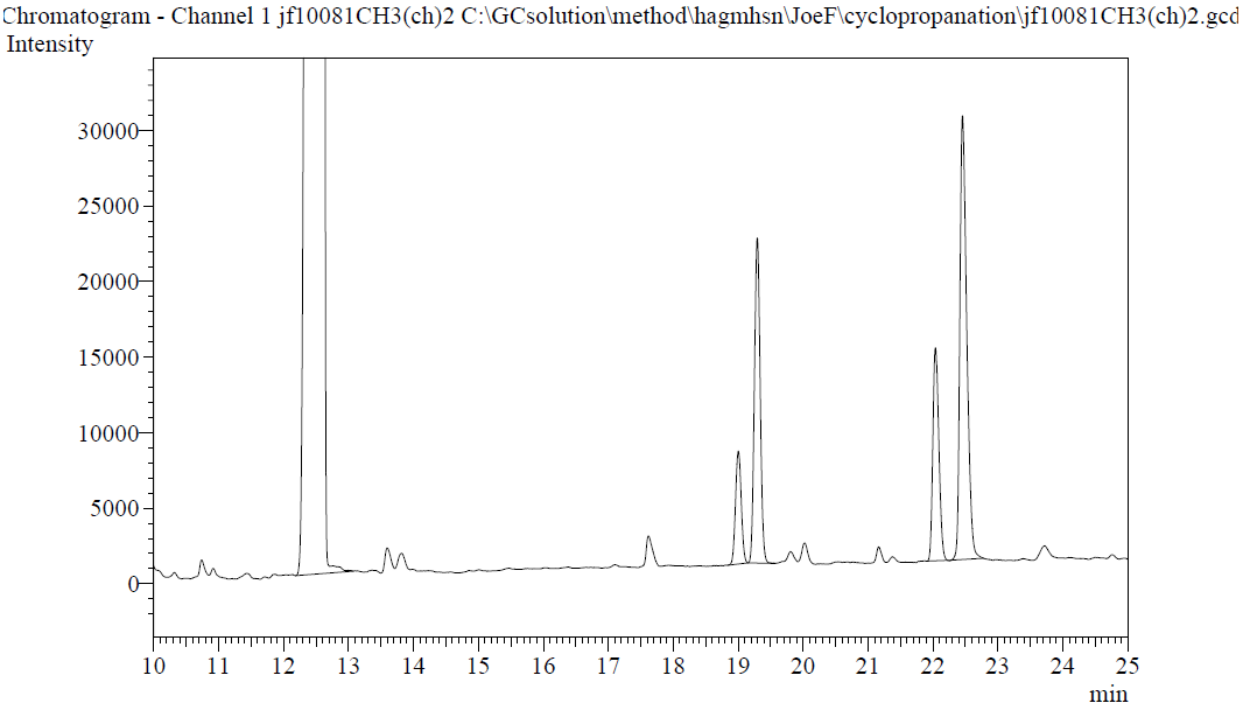

Figure S20. Cyclopropantion of 1,3-pentadiene catalyzed by CMOF-**1R**. *Cis* e.e.: 49%; *trans* e.e.: 40%; yield: 11%; d.r. 1.7.

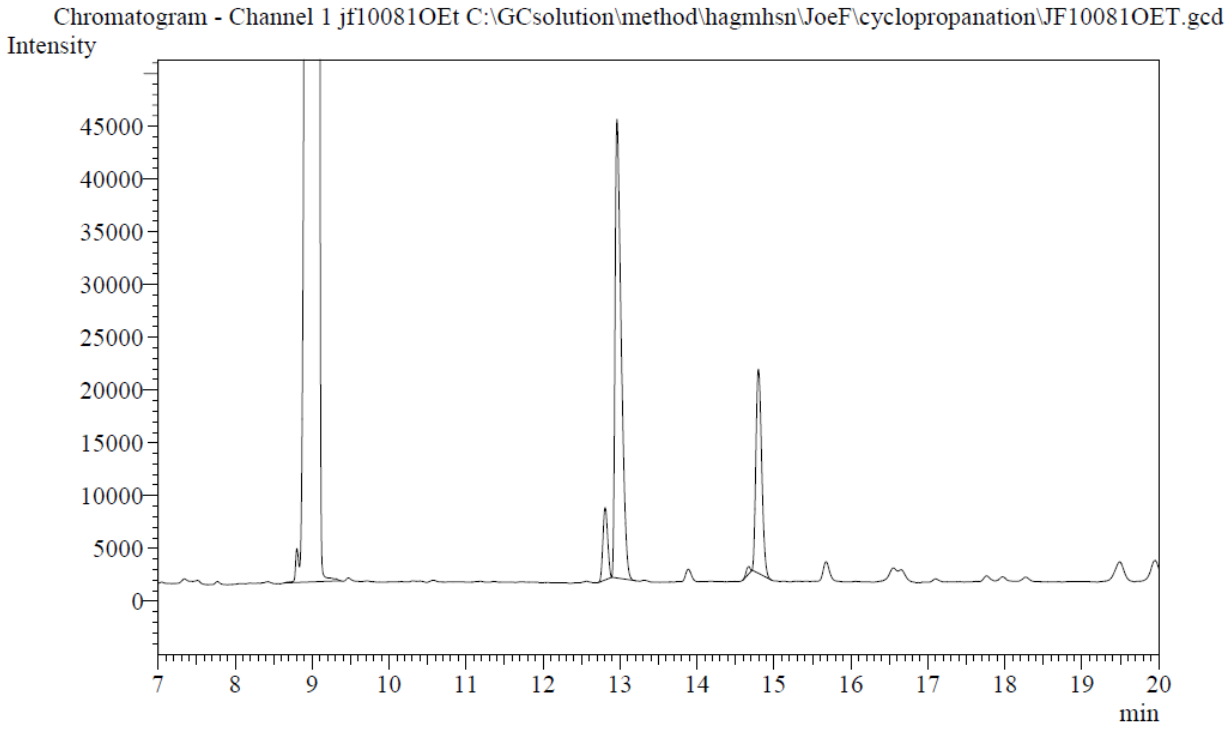

Figure S21. Cyclopropanation of ethyl vinyl ether catalyzed by CMOF-**1R**. *Cis* e.e.: 95%; *trans* e.e.: 79%; yield: 22%; d.r.: 2.6.

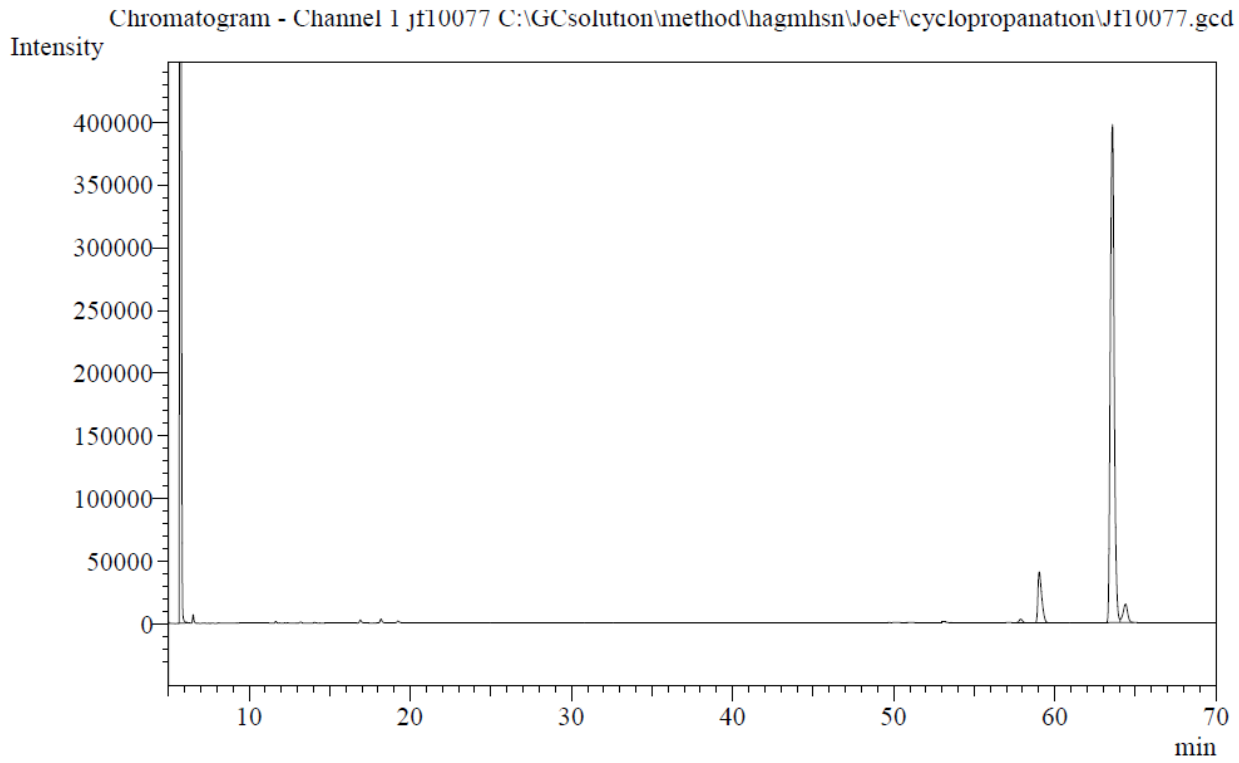

Figure S22. Cyclopropanation of styrene catalyzed by CMOF-**2R**. *Trans* e.e.: 94%; *cis* e.e.: 92%; yield: 55%; d.r.: 9.6.

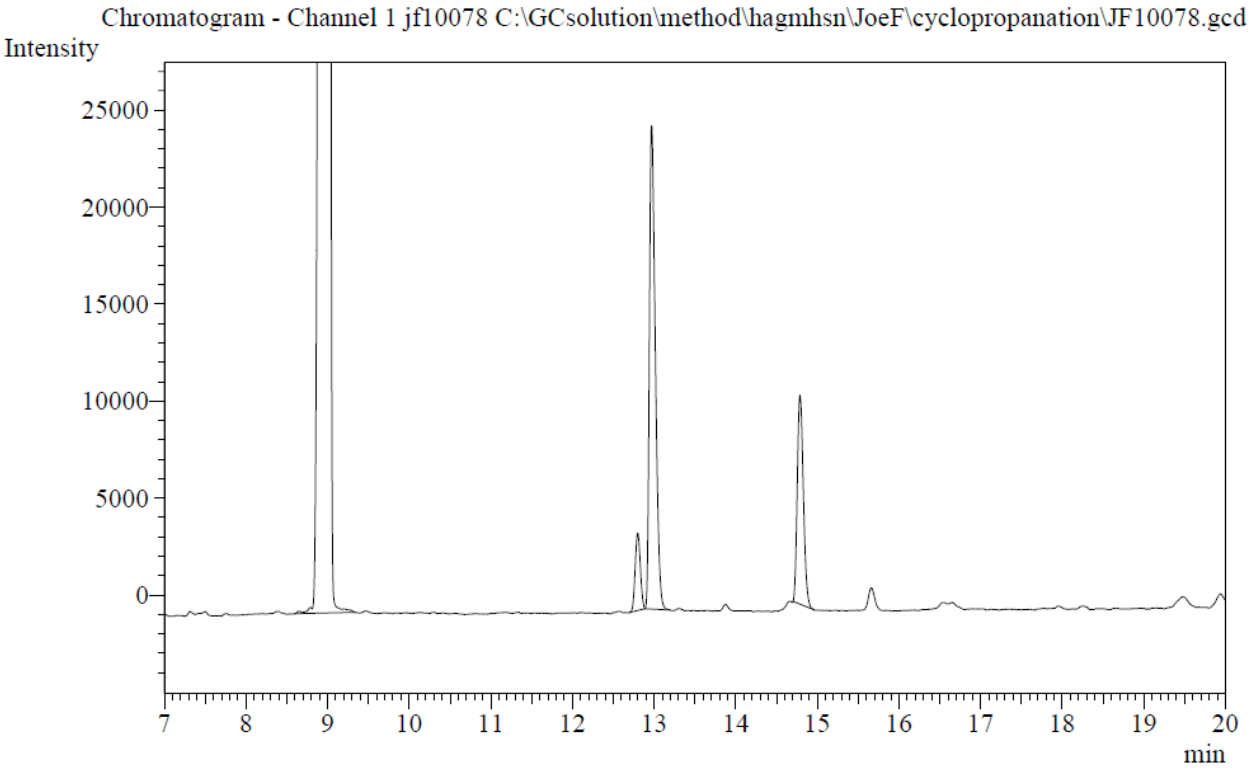

Figure S23: Cyclopropanation of ethyl vinyl ether catalyzed by CMOF-**2R**. *Trans* e.e.: 76%; *cis* e.e.: >99%; yield: 22%; d.r.: 2.6.

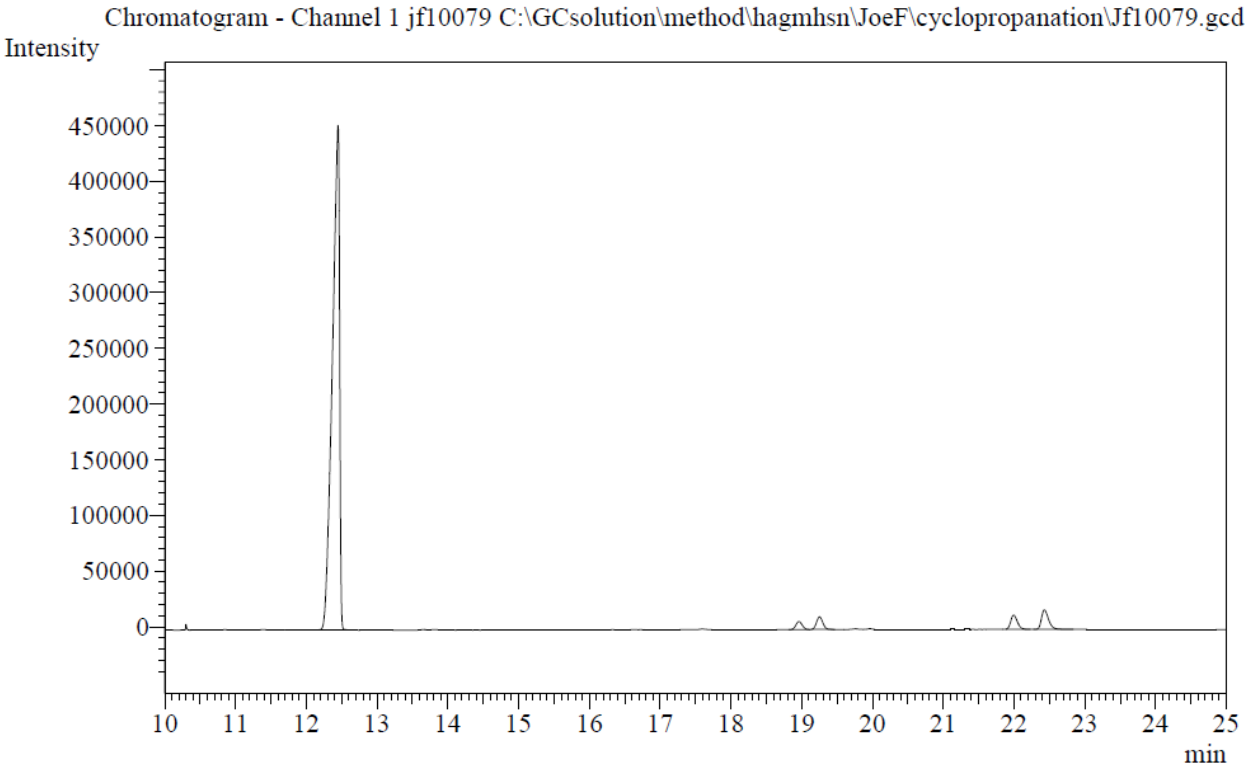

Figure S24. Cyclopropanation of 1,3-pentadiene catalyzed by CMOF-**2R**. *Cis* e.e.: 21%; *trans* e.e.: 19%; yield: 18.5%; d.r.: 1.8.

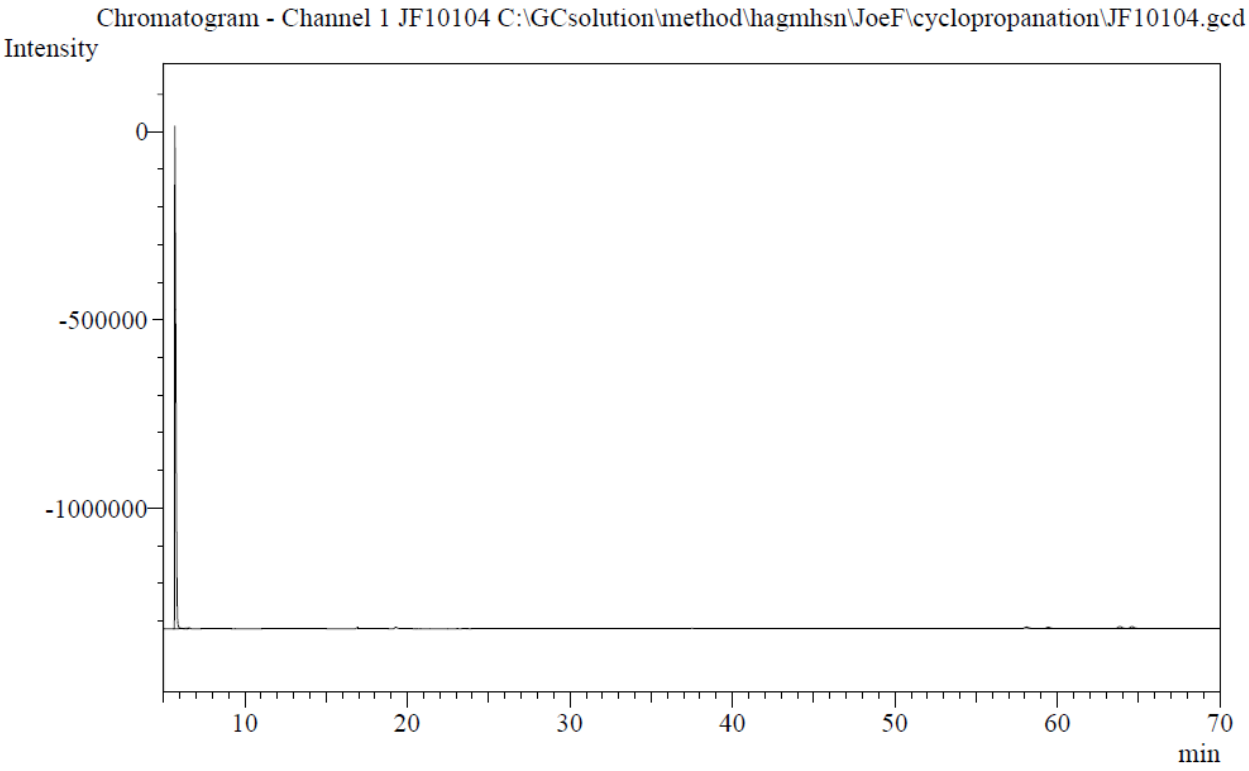

Figure S25. Cyclopropanation of styrene catalyzed by CMOF-2 without the addition of $NaB(OMe)_3H$ *Cis* e.e.: 34%; *trans* e.e.: 0%; yield: <2%; d.r.: 2.3.

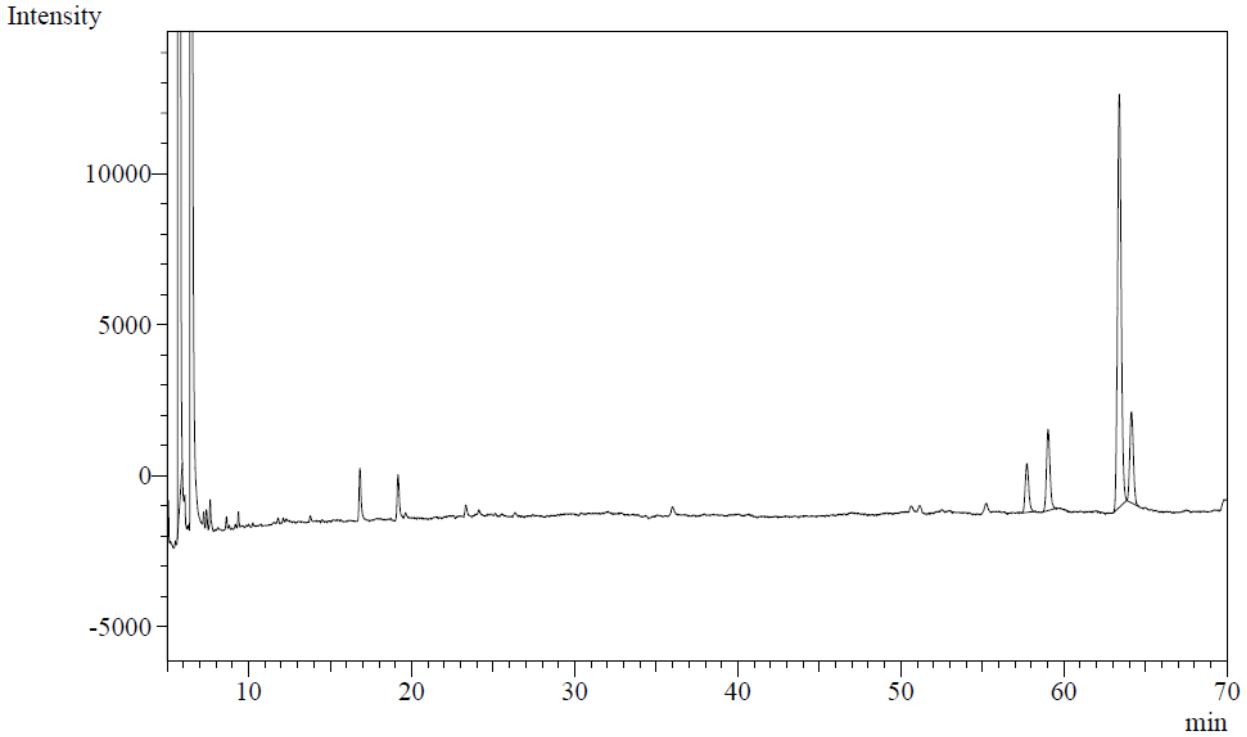

Figure S26. Cyclopropanation of styrene catalyzed by CMOF-2 after 3 hours. *Cis* e.e.: 25%; *trans* e.e.: 64.5%; yield: 3%; d.r.: 4.0.

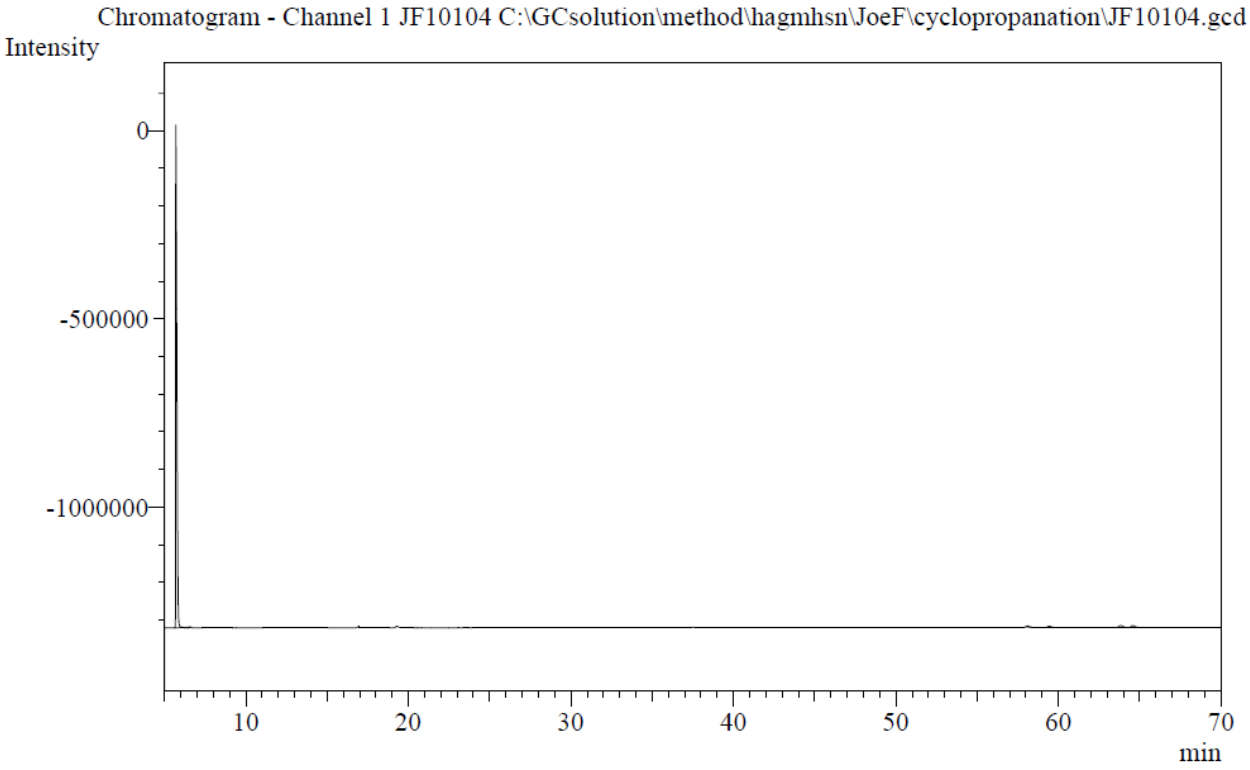

Figure S27. Cyclopropanation of styrene catalyzed by CMOF-2 supernatant 12 hours after filtration. *Cis* e.e.: 32%; *trans* e.e.: 66%; yield: 3%; d.r.: 4.0.

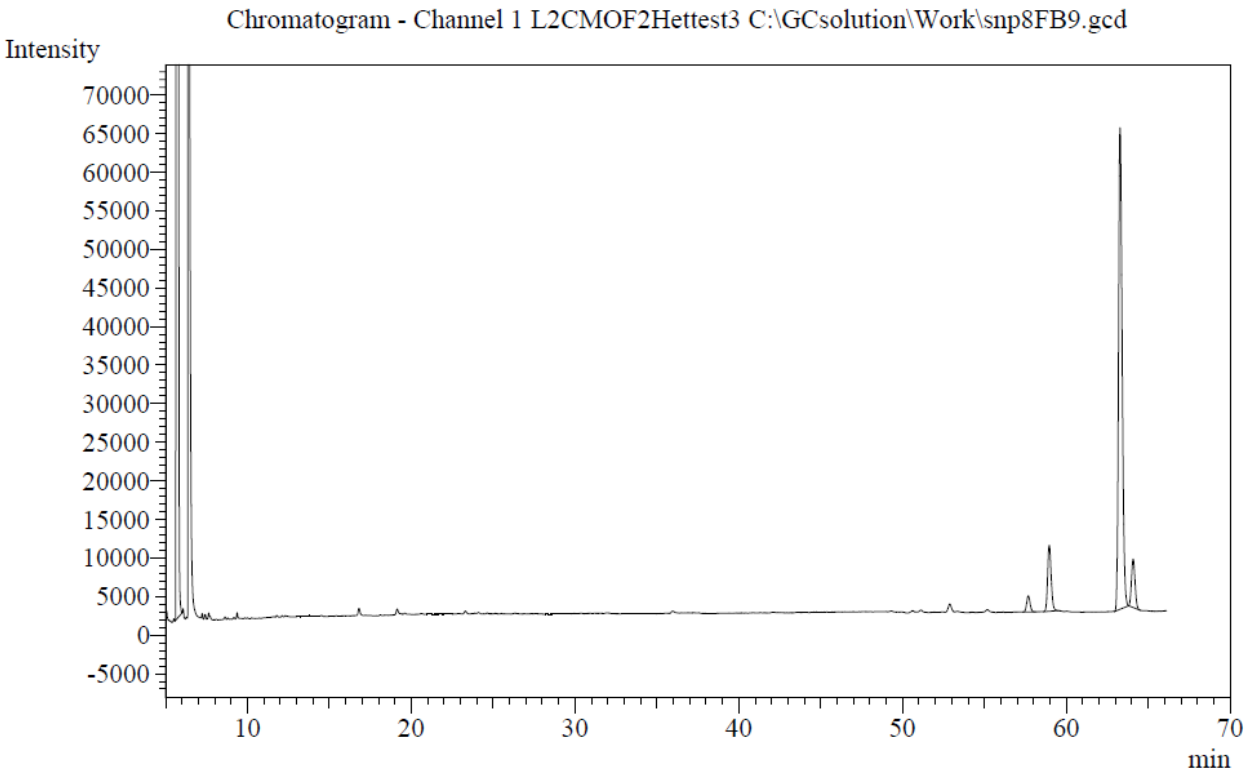

Figure S28. Cyclopropanation of styrene catalyzed by CMOF-2 after 15 hours. *Cis* e.e.: 62%; *trans* e.e.: 82%; yield: 9%; d.r.: 6.6.

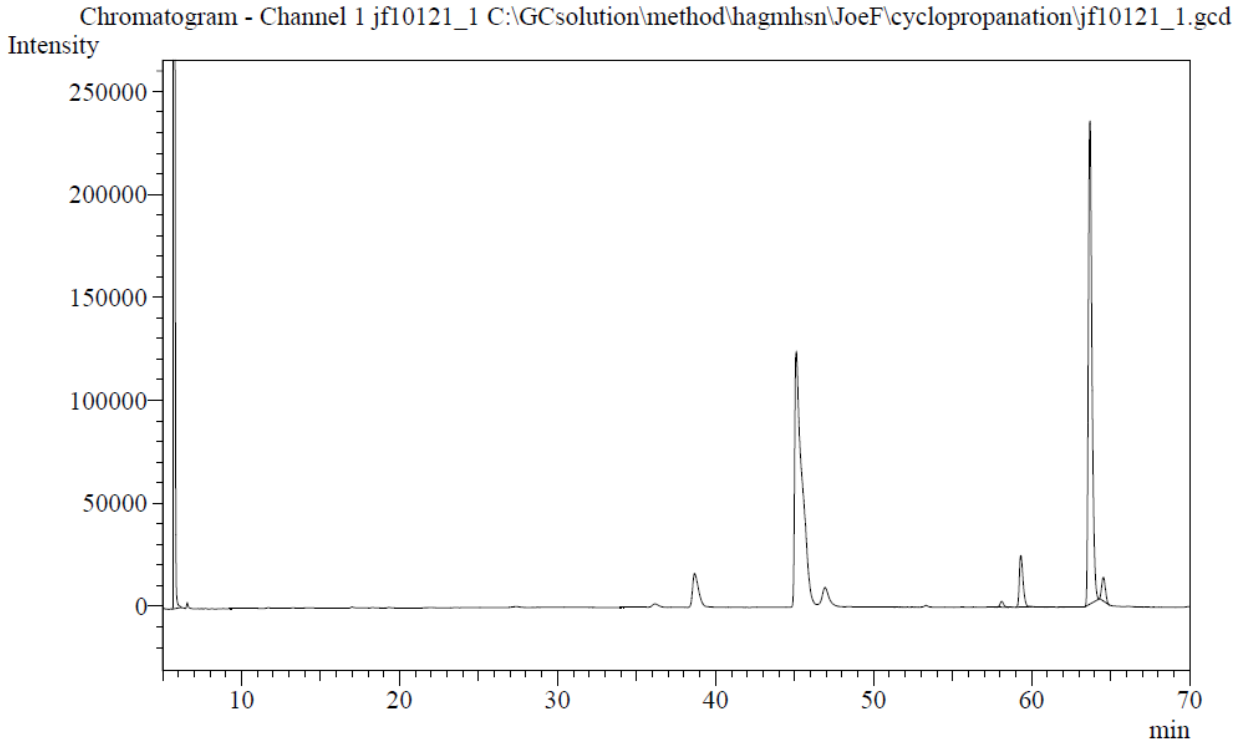

Figure S29. Cyclopropanation of styrene catalyzed by CMOF-**2**. First use: *Cis* e.e.: 82%; *trans* e.e.: 91%; yield: 47%; d.r.: 8.8.

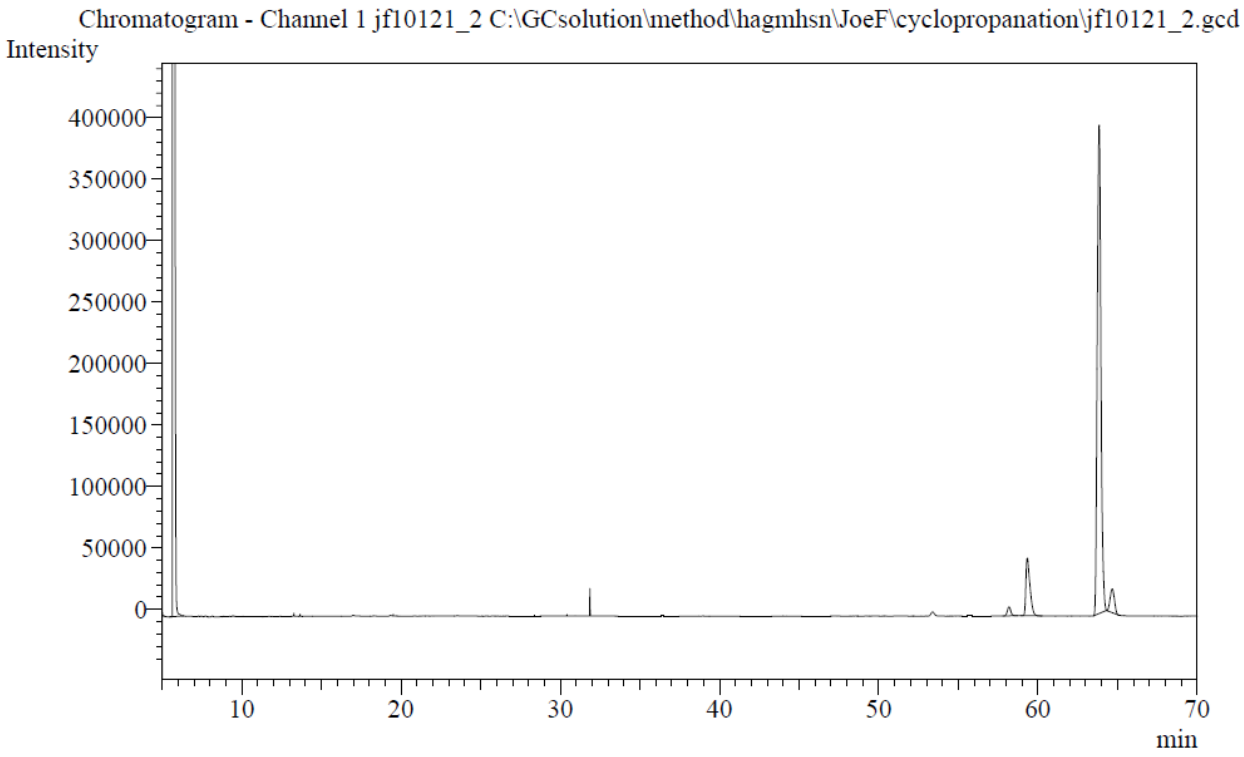

Figure S30. Cyclopropanation of styrene catalyzed by CMOF-2. Second use: *Cis* e.e.: 77%; *trans* e.e.: 89%; yield: 35%; d.r.: 7.1

Reference

1. Song, F.; Wang, C.; Falkowski, J. M.; Ma, L.; Lin, W. *J. Am. Chem. Soc.* **2010**, *132*, 15390-15398.